Supplementary Information for

Conjugated cyclized-polyacrylonitrile encapsulated carbon nanotubes as core-sheath heterostructured anodes with favorable lithium storage

Qian Liu,[‡a] Zongyin Xiao,[‡a] Xun Cui,[bc] Shuyi Deng,[c] Qiming He,[a] Qing Zhang,[a] Zhiqun Lin,[*b] and Yingkui Yang[*ac]

[a] *Key Laboratory of Catalysis and Energy Materials Chemistry of Ministry of Education & Hubei Key Laboratory of Catalysis and Materials Science, South-Central University for Nationalities, Wuhan 430074, China*

E-mail: ykyang@mail.scuec.edu.cn

[b] *School of Materials Science and Engineering, Georgia Institute of Technology, Atlanta, GA 30332, USA*

E-mail: zhiqun.lin@mse.gatech.edu

[c] *Hubei Engineering Technology Research Centre of Energy Polymer Materials, School of Chemistry and Materials Science, South-Central University for Nationalities, Wuhan 430074, China*

[‡] *These two authors equally contributed to this work.*

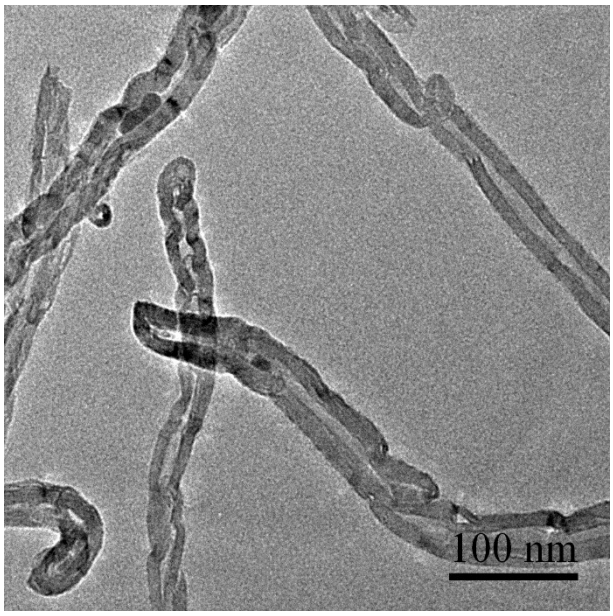

Fig. S1 Typical TEM image of bare CNTs.

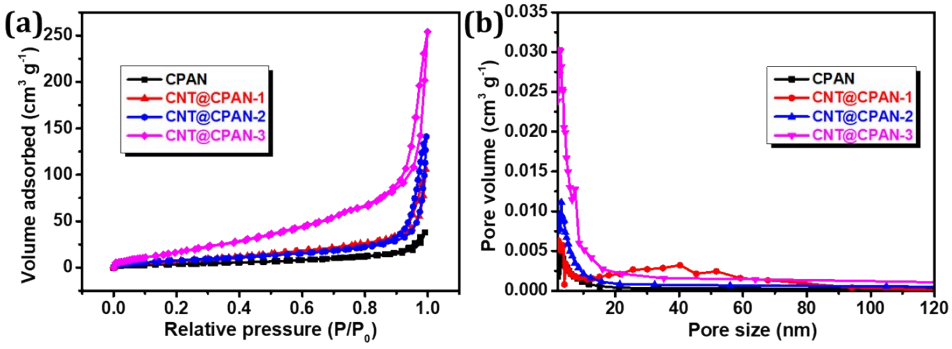

Fig. S2 N_2 adsorption/desorption isotherms and (b) pore size distributions of CPAN and its composites.

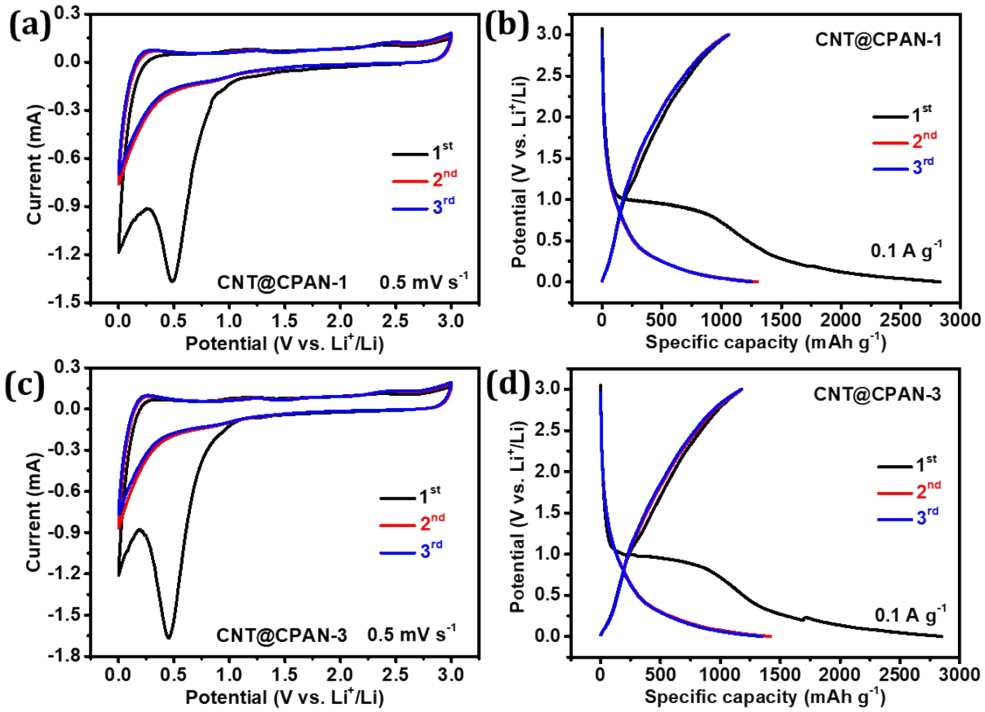

Fig. S3 Typical CV curves of (a) CNT@CPAN-1 and (c) CNT@CPAN-3 at 0.5 mV s^{-1}, and charge/discharge curves of (b) CNT@CPAN-1 and (d) CNT@CPAN-3 at 0.1 A g^{-1} in the first three cycles.

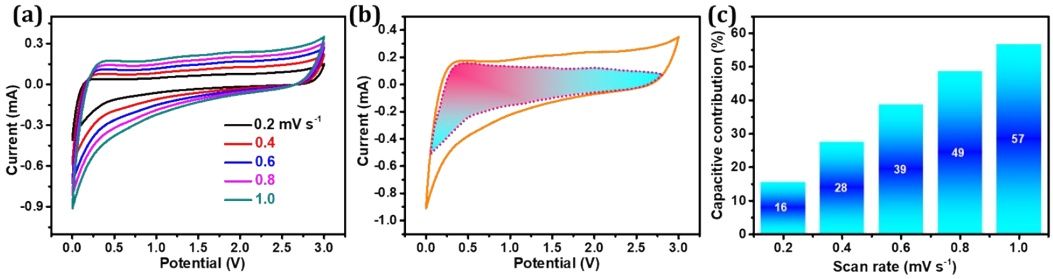

Fig. S4 CPAN anode: (a) CV curves at scan rates from 0.2 to 10 mV s^{-1}, (b) the decoupling of capacitive contribution (shadow) at 1 mV s^{-1}, and (c) the normalized capacitive contribution at different scan rates.

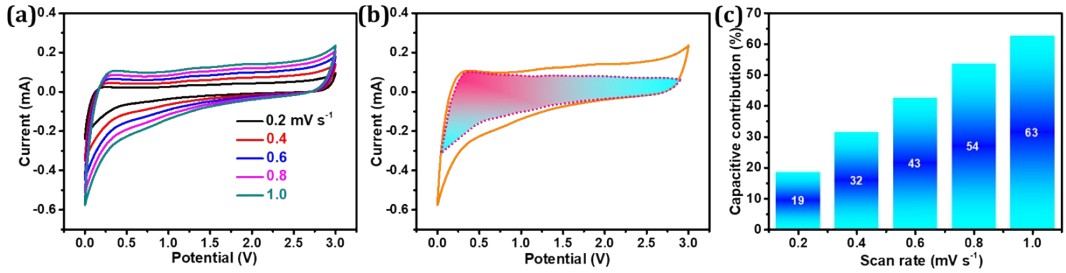

Fig. S5 CNT@CPAN-1 anode: (a) CV curves at scan rates from 0.2 to 10 mV s^{-1}, (b) the decoupling of capacitive contribution (shadow) at 1 mV s^{-1}, and (c) the normalized capacitive contribution at different scan rates.

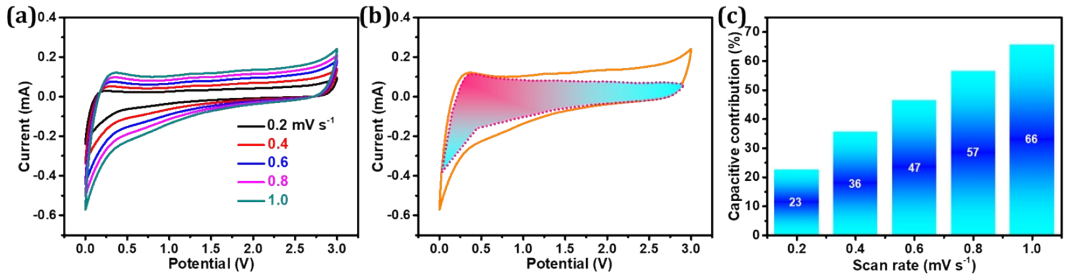

Fig. S6 CNT@CPAN-2 anode: (a) CV curves at scan rates from 0.2 to 10 mV s^{-1}, (b) the decoupling of capacitive contribution (shadow) at 1 mV s^{-1}, and (c) the normalized capacitive contribution at different scan rates.

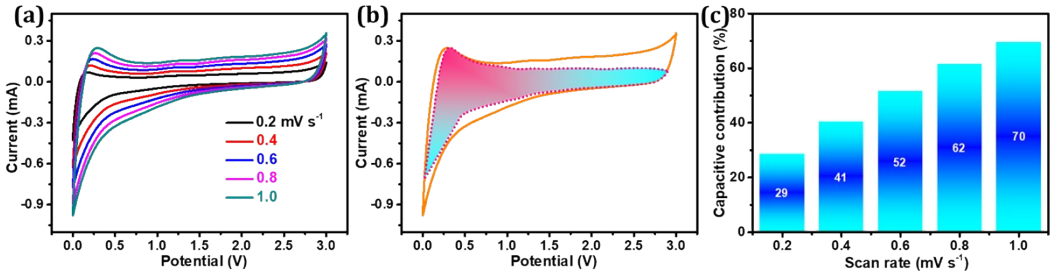

Fig. S7 CNT@CPAN-3 anode: (a) CV curves at scan rates from 0.2 to 10 mV s^{-1}, (b) the decoupling of capacitive contribution (shadow) at 1 mV s^{-1}, and (c) the normalized capacitive contribution at different scan rates.

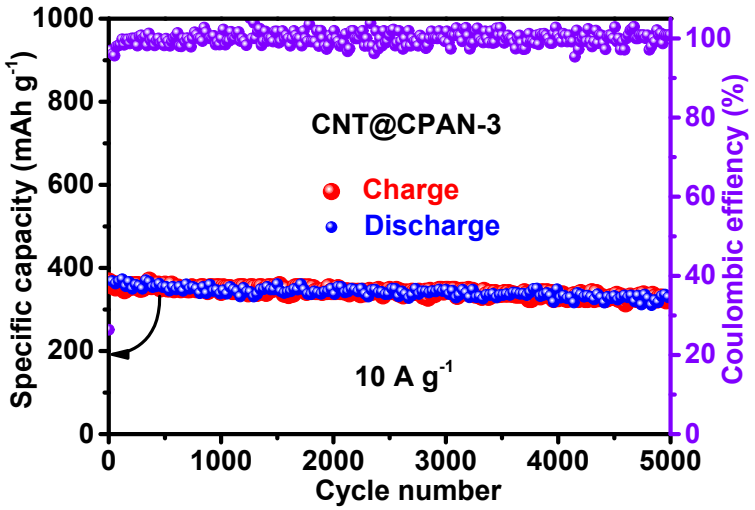

Fig. S8 Long-term cycle life and the corresponding coulombic efficiency of CNT@CPAN-3 at a high rate of 10 A g^{-1} for 5000 cycles.

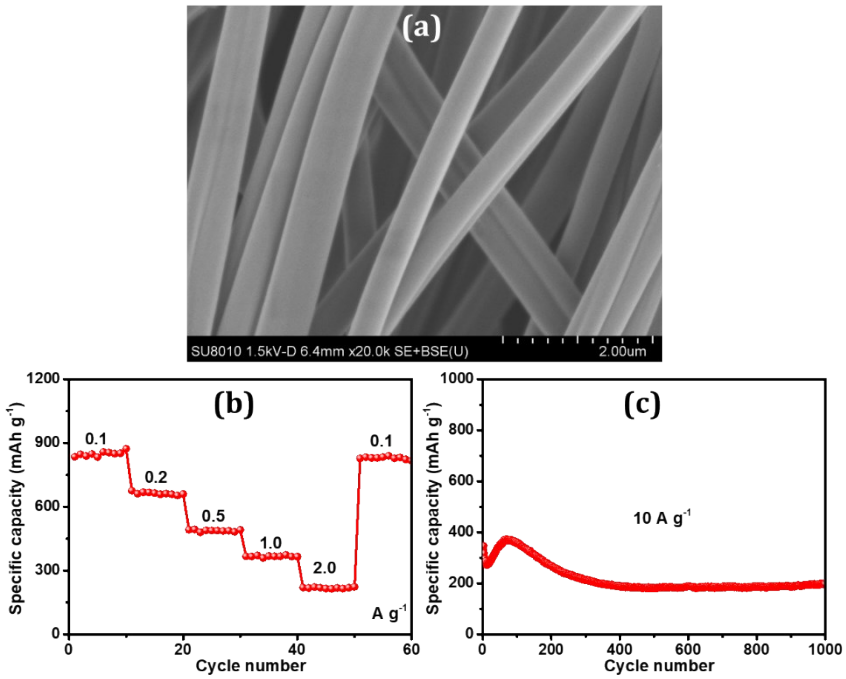

Fig. S9 (a) SEM images of the electrospun CPAN fibers derived from the as-synthesized PAN; (b) reversible capacity at different rates, and (c) cycling stability at 10 A g^{-1} for 1000 cycles.

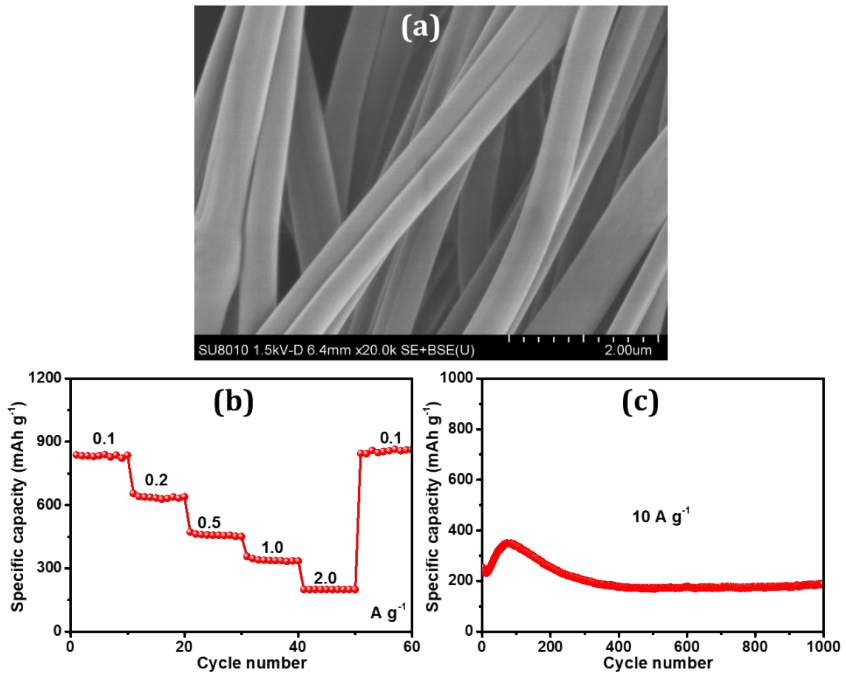

Fig. S10 (a) SEM image of electrospun CPAN fibers using commercial polyacrylonitrile precursor; (b) reversible capacity at different rates, and (c) cycling stability at 10 A g^{-1} for 1000 cycles.

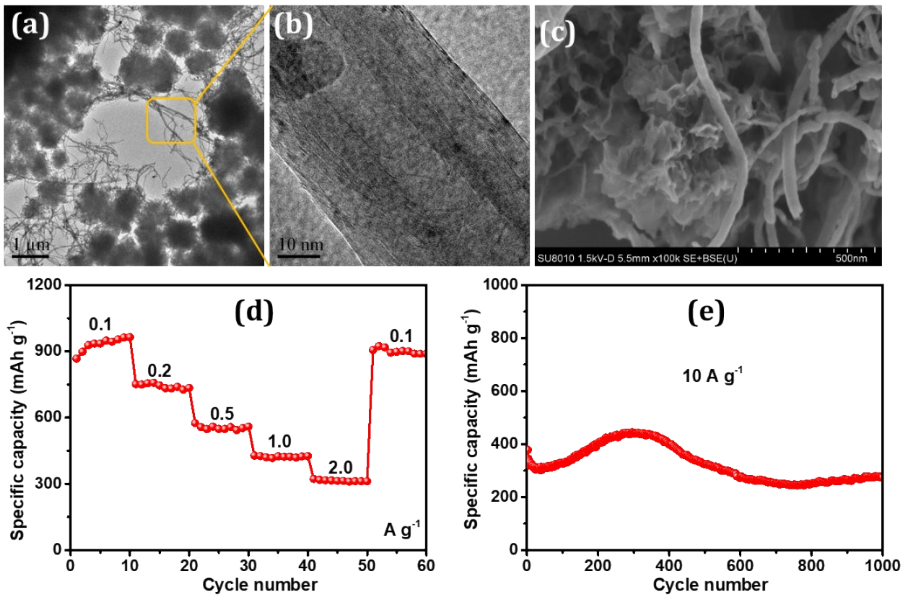

Fig. S11 TEM (a) and (c) SEM images of the mixture of CPAN and CNTs where (b) CNTs are totally exposed without covering by CPAN; (d) reversible capacity at different rates, and (e) cycling stability at 10 A g^{-1} for 1000 cycles.

Table S1 Lithium storage performance of selected CNT@CPAN-3 anode and polymer-based anode counterparts reported in the references

Polymers used	Specific capacity	Rate capability	Cycling stability	Ref.
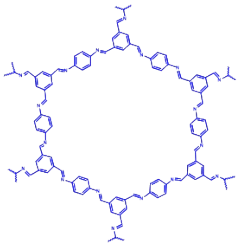	125 mAh g^{-1} at 100 mA g^{-1}	—	77.3% after 300 cycles at 100 mA g^{-1}	[1]
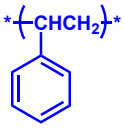	149.97 mAh g^{-1} at 100 mA g^{-1}	90.38 mAh g^{-1} at 0.5 A g^{-1}	67.6% after 300 cycles at 100 mA g^{-1}	[2]
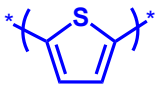	745 mAh g^{-1} at 45 mA g^{-1}	141 mAh g^{-1} at 3.0 A g^{-1}	30% after 300 cycles at 100 mA g^{-1}	[3]
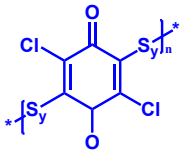	85 mAh g^{-1} at 100 mA g^{-1}	99 mAh g^{-1} at 1.0 A g^{-1}	67% after 200 cycles at 200 mA g^{-1}	[4]
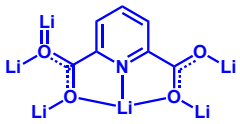	160 mAh g^{-1} at 30 mA g^{-1}	—	57.1% after 50 cycles at 30 mA g^{-1}	[5]
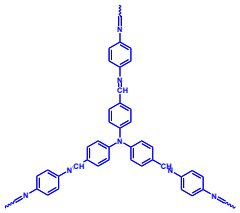	140 mAh g^{-1} at 0.4 C	60 mAh g^{-1} at 16 C	—	[6]
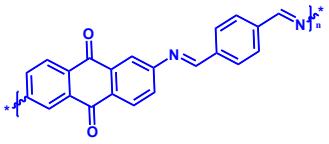	1401 mAh g^{-1} at 100 mA g^{-1}	259 mAh g^{-1} at 2.0 A g^{-1}	97% after 1000 cycles at 200 mA g^{-1}	[7]
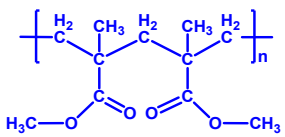	206 mAh g^{-1} at 20 mA g^{-1}	167 mAh g^{-1} at 0.4 A g^{-1}	~100% after 1000 cycles at 400 mA g^{-1}	[8]
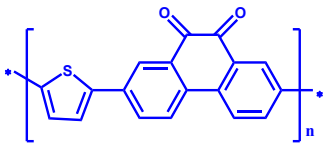	387 mAh g^{-1} at 72 mA g^{-1}	155 mAh g^{-1} at 0.72 A g^{-1}		[9]

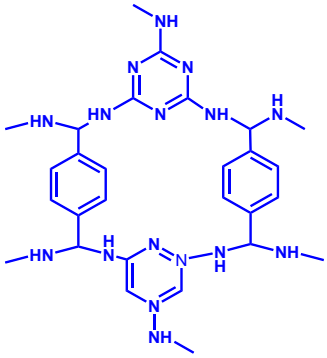	761 mAh g^{-1} at 100 mA g^{-1}	299 mAh g^{-1} at 2.0 A g^{-1}	—	[10]
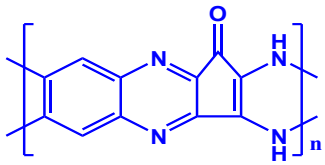	972 mAh g^{-1} at 100 mA g^{-1}	419 mAh g^{-1} at 2.0 A g^{-1}	87.8% after 1000 cycles at 2500 mA g^{-1}	[11]
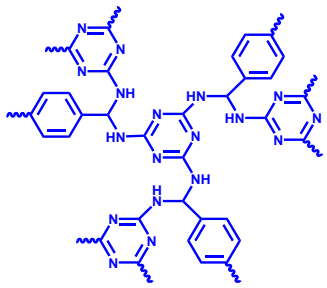	50 mAh g^{-1} at 50 mA g^{-1}	15 mAh g^{-1} at 10 A g^{-1}	—	[12]
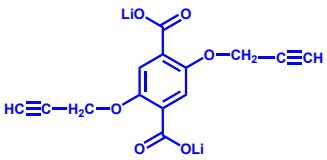	175 mAh g^{-1} at 0.1 C	140 mAh g^{-1} at 2.0 C	—	[13]
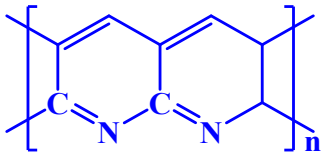	**1176 mAh g^{-1} at 100 mA g^{-1}**	**439 mAh g^{-1} at 2.0 A g^{-1}**	**94% after 5000 cycles at 10 A g^{-1}**	***This work***

References

[1] Z. D. Lei, Q. Yang, Y. Xu, S. Y. Guo, W. W. Sun, H. Liu, L.-P. Lv, Y. Zhang and Y. Wang, *Nat. Commun.*, 2018, **9**, 576.

[2] Y. Aldawsari, Y. Mussa, F. Ahmed, M. Arsalan and E. Alsharaeh, *Materials*, 2019, **12**, 2248.

[3] C. Zhang, Y. W. He, P. Mu, X. Wang, Q. He, Y. Chen, J. H. Zeng, F. Wang, Y. H. Xu and J. X. Jiang, *Adv. Funct. Mater.*, 2018, **28**, 1705432.

[4] L. L. Cai, Y. H. Wen, J. Cheng, G. P. Cao and Y. S. Yang, *Acta Phys-Chim. Sin.*, 2016, **32**, 969-974.

[5] L. Gou, H. X. Zhang, X. Y. Fan and D. L. Li, *Inorg. Chim. Acta*, 2013, **394**, 10-14.

[6] Y. B. Sun, Y. H. Sun, Q. Y. Pan, G. Li, B. Han, D. L. Zeng, Y. F. Zhang and H. S. Cheng, *Chem. Commun.*, 2016, **52**, 3000-3002.

[7] Z. M. Man, P. Li, D. Zhou, R. Zang, S. J. Wang, P. X. Li, S. S. Liu, X. M. Li, Y. H. Wu, X. H. Liang and G. X. Wang, *J. Mater. Chem. A*, 2019, **7**, 2368-2375.

[8] Z. F. Sha, S. Q. Qiu, Q. Zhang, Z. Y. Huang, X. Cui, Y. K. Yang, Z. Q. Lin, J. Mater. Chem. A, 2019, **7**, 23019-23027.

[9] Q. Yuan, C. X. Li, X. Guo, J. S. Zhao, Y. Zhang, B. Wang, Y. Y. Dong and L. X. Liu, Energy Reports, 2020, **6**, 2094-2105.

[10] Z. D. Lei, X. D. Chen, W. W. Sun, Y. Zhang and Y. Wang, Adv. Energy Mater., 2018, **9**, 1801010.

[11] J. Xie, X. H. Rui, P. Y. Gu, J. S. Wu, Z. C. J. Xu, Q. Y. Yan and Q. C. Zhang, ACS Appl. Mater. Interfaces, 2016, **8**, 16932-16938.

[12] S. X. Xu, W. Xu, L. J. Kong and Y. H. Zhang, SN Appl. Sci., 2020, **2**, 2523-3963.

[13] S. N. Zhang, S. Ren, D. M. Han, M. Xiao, S. J. Wang, L. Y. Sun and Y. Z. Meng, ACS Appl. Mater. Interfaces., 2020, **12**, 36237-36246.